Lumped Capacitance, Open-Circuit End Effects, and Edge-Capacitance of Microstrip-Like Transmission Lines for Microwave and Millimeter-Wave Applications

BHARATHI BHAT, SENIOR MEMBER, IEEE, AND SHIBAN KISHEN KOUL, MEMBER, IEEE

Abstract—**A detailed analysis of lumped capacitance, open-circuit end effects, and edge-capacitance of finite-length strip conductors embedded in multilayer, isotropic dielectrics without sidewalls is presented. The analysis uses the well-known variational technique, in conjunction with the transverse transmission-line technique. The lumped capacitances of square and rectangular conductor patches in sandwiched microstrip, inverted microstrip, and suspended microstrip are computed. Further, extensive data on the open-circuit end effects and edge-capacitances of finite-length strip conductors in these microstrip-like transmission lines are generated. Using the method presented, the analysis of lumped capacitance, open-circuit end effects, and edge-capacitances of finite-length strip conductors in various microstrip-like structures reduces to the determination of a single admittance parameter. This parameter can be simply obtained from the transmission-line equivalent circuit.**

I. Introduction

THE CONVENTIONAL microstrip transmission line has been extensively used in fabricating various circuit components at microwave frequencies [1]. Some of its modified versions, namely, the sandwiched microstrip, inverted microstrip, and suspended microstrip, have proven useful at higher microwave and millimeter-wave frequencies [2], [3]. The propagation parameters, i.e., the characteristic impedance, the effective dielectric constant, and the phase velocity of the aforementioned microstrip-like transmission lines, have been extensively analyzed in the literature. For some specific circuit applications, a knowledge of the lumped capacitance and open-circuit end effects of finite-length strip conductors in these microstrip-like configurations is essential.

There are a limited number of papers available in the literature on the lumped capacitance, open-circuit end effects, and edge-capacitance of the conventional microstrip configuration. The quasi-static analysis using the method of moments has been reported by Farrar and Adams [4]. Itoh *et al.* [5] studied the end effects of open microstrip structures using the Galerkin's method in the Fourier-transform domain. A closed-form expression for the open-end discontinuity capacitance in shielded microstrip has been reported by Bedair and Sobhy [6]. Their results are based on the results obtained earlier for the stripline configuration [7]. The analysis of edge-capacitance in shielded microstrip using the variational method in the space-domain has been reported by Maeda [8]. The most extensive data on the microstrip open-circuit has been given by Silvester and Benedek [9] using the method of line sources with charge reversal. They have also given an empirical expression, which is very useful for computational purposes. Some results on the microstrip end effects have also been reported by James and Tse [10]. The hybrid-mode analysis of microstrip end effects has been reported by Hornsby [11] and Jansen [12]. The experimental investigations on the end effects have been carried out by Napoli and Hughes [13], Easter *et al.* [14], and James and Tse [10].

Except for one graph on the end effects of suspended substrate line [12], there is no design information available in the open literature on the lumped capacitance, open-circuit end effects, and edge-capacitance of various modified versions of the conventional microstrip.

In this paper, the lumped capacitance, open-circuit end effects, and edge-capacitance of a layered microstrip structure are analyzed using the variational method in conjunction with the transverse transmission-line technique. Extensive design data on the lumped capacitances of square and rectangular conductor patches in sandwiched microstrip, inverted microstrip, and suspended microstrip are numerically generated. The data on open-circuit end effects and edge-capacitances in these transmission lines are also computed. The technique presented is quite simple and general. Determination of a single parameter, namely, the admittance at the charge plane, is sufficient to analyze the lumped capacitance, open-circuit end effects, and edge-capacitance of a variety of microstrip-like transmission lines.

II. Analysis

Consider a strip conductor of finite length sandwiched between four-layer isotropic dielectrics as shown in Fig. 1. The dielectric structure extends to infinity in the $\pm x$ and

Manuscript received August 24, 1983; revised November 7, 1983.

The authors are with the Centre for Applied Research in Electronics, Indian Institute of Technology, Hauz Khas, New Delhi-110016, India.

0018-9480/84/0300-0433$01.00 ©1984 IEEE

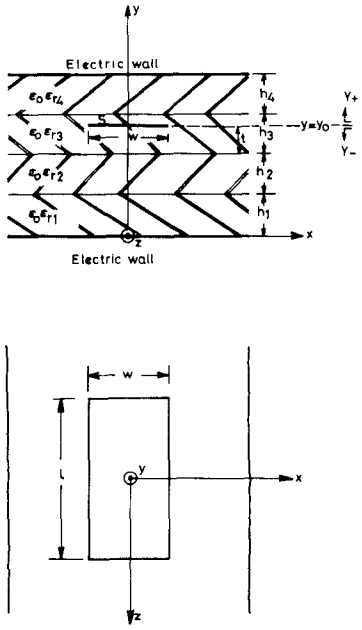

Fig. 1. Finite-length strip conductor embedded in four-layer isotropic dielectric structure.

$\pm z$ directions. The variational expression for the line capacitance of an infinitely thin strip conductor of finite length in the Fourier transform domain can be written as

$$\frac{1}{C_l} = \frac{1}{(2\pi)^2 Q^2} \int_{-\infty}^{\infty} \int_{-\infty}^{\infty} \phi(\alpha, y_0, \beta) f(\alpha, \beta)\, d\alpha\, d\beta \quad (1)$$

where Q is the total charge on the strip conductor S, $f(\alpha, \beta)$ is the Fourier transform of the charge distribution $f(x, z)$ on the strip conductor S in the $x-z$ plane, and $\phi(\alpha, y_0, \beta)$ is the Fourier transform of the potential distribution function $\phi(x, y, z)$ at the charge plane $y = y_0$. These quantities are given by

$$Q = \iint_S f(x, z)\, dx\, dz \quad (2)$$

$$f(\alpha, \beta) = \int_{-\infty}^{\infty} \int_{-\infty}^{\infty} f(x, z) e^{j(\alpha x + \beta z)}\, dx\, dz \quad (3)$$

$$\phi(\alpha, y, \beta) = \int_{-\infty}^{\infty} \int_{-\infty}^{\infty} \phi(x, y, z) e^{j(\alpha x + \beta z)}\, dx\, dz. \quad (4)$$

To determine the capacitance of a finite-length strip conductor sandwiched between multilayer dielectrics using (1), $\phi(\alpha, y_0, \beta)$ has to be determined and a suitable charge distribution $f(x, z)$ on the strip conductor has to be assumed. The potential distribution function satisfies the Poisson's differential equation

$$\nabla^2 \phi(x, y, z) = -\left(\frac{1}{\epsilon}\right) f(x, z) \delta(y - y_0). \quad (5)$$

Fourier transforming (5) with respect to x and z, we get

$$\left[\frac{d^2}{dy^2} - \xi^2\right] \phi(\alpha, y, \beta) = -\left(\frac{1}{\epsilon}\right) f(\alpha, \beta) \delta(y - y_0) \quad (6)$$

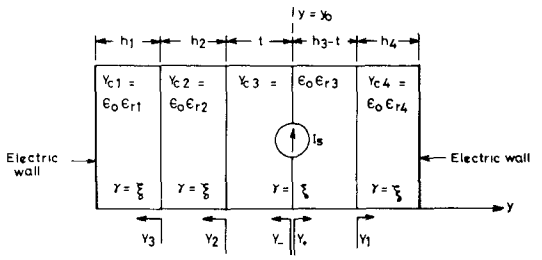

Fig. 2. Two-wire transmission-line equivalent of the structure shown in Fig. 1.

where

$$\xi^2 = \alpha^2 + \beta^2 \quad (7)$$

and ϵ is the absolute dielectric constant of the medium.

The boundary conditions at the various dielectric interfaces are given by

$$\phi\left(\alpha, \sum_{l=1}^{J} h_l - 0, \beta\right) = \phi\left(\alpha, \sum_{l=1}^{J} h_l + 0, \beta\right) \quad (8)$$

$$\epsilon_0 \epsilon_{rJ} \frac{d}{dy} \phi\left(\alpha, \sum_{l=1}^{J} h_l - 0, \beta\right) = \epsilon_0 \epsilon_{rJ+1} \frac{d}{dy} \phi\left(\alpha, \sum_{l=1}^{J} h_l + 0, \beta\right), \qquad j = 1, 2, 3, 4. \quad (9)$$

In order to solve for $\phi(\alpha, y, \beta)$, we use the transverse transmission-line method [2]. For a transmission line with a current source of intensity I_s located at $y = y_0$ (Fig. 2), the voltage V along the line satisfies the differential equation

$$\left[\frac{d^2}{dy^2} - \gamma^2\right] V = -\gamma Z_c I_s \delta(y - y_0). \quad (10)$$

Further, the continuity conditions at the interfaces are given by

$$V_j = V_{j+1} \quad (11)$$

and

$$Y_{cJ} \frac{dV_J}{dy} = Y_{cJ+1} \frac{dV_{J+1}}{dy}, \qquad j = 1, 2, 3, 4 \quad (12)$$

where γ is the propagation constant, Z_c is the characteristic impedance in general, and Y_{cJ} is the characteristic admittance of the jth section of the transmission line. Comparing (6)–(9) with (10)–(12), we get the following analogous relations:

$$V = \phi(\alpha, y, \beta), \gamma = \xi = \sqrt{\alpha^2 + \beta^2}, \quad Z_c = \frac{1}{\epsilon}, \quad I_s = \frac{f(\alpha, \beta)}{\xi}$$

$$Y_{cJ} = \epsilon_0 \epsilon_{rJ}. \quad (13)$$

Since $V = I_s / Y$ at $y = y_0$, we have

$$\phi(\alpha, y_0, \beta) = \frac{f(\alpha, \beta)}{\left(\sqrt{\alpha^2 + \beta^2}\right) Y} \quad (14)$$

where Y, the admittance at the charge plane $y = y_0$, is obtained from the transmission-line equivalent circuit

shown in Fig. 2. This expression is given by

$$Y = Y_+ + Y_- \tag{15a}$$

$$Y_+ = \epsilon_0\epsilon_{r3}\left[\left(Y_1 + \epsilon_0\epsilon_{r3}\tanh\left(\xi(h_3 - t)\right)\right)/ \cdot\left(\epsilon_0\epsilon_{r3} + Y_1\tanh\left(\xi(h_3 - t)\right)\right)\right] \tag{15b}$$

$$Y_- = \epsilon_0\epsilon_{r3}\left[\left(Y_2 + \epsilon_0\epsilon_{r3}\tanh\left(\xi t\right)\right)/\left(\epsilon_0\epsilon_{r3} + Y_2\tanh\left(\xi t\right)\right)\right] \tag{15c}$$

$$Y_1 = \epsilon_0\epsilon_{r4}\coth\left(\xi h_4\right) \tag{15d}$$

$$Y_3 = \epsilon_0\epsilon_{r1}\coth\left(\xi h_1\right) \tag{15e}$$

$$Y_2 = \epsilon_0\epsilon_{r2}\left[\left(Y_3 + \epsilon_0\epsilon_{r2}\tanh\left(\xi h_2\right)\right)/\left(\epsilon_0\epsilon_{r2} + Y_3\tanh\left(\xi h_2\right)\right)\right]. \tag{15f}$$

Combining (1) and (14), we get

$$\frac{1}{C_l} = \frac{1}{4\pi^2}\int_{-\infty}^{\infty}\int_{-\infty}^{\infty}\left[\frac{f(\alpha,\beta)}{Q}\right]^2 \frac{1}{\sqrt{(\alpha^2+\beta^2)}\,Y}\,d\alpha\,d\beta. \tag{16}$$

The charge distribution on the strip conductor can be rewritten as

$$f(x,z) = f(x)g(z) \tag{17}$$

where $f(x)$ and $g(z)$ specify the variations in the x- and z-directions, respectively. For the x-direction, we assume a charge distribution similar to that used by the authors for a uniform line [2]

$$f(x) = \begin{cases} 1 + \left|\dfrac{2x}{w}\right|^3, & -w/2 \leqslant x \leqslant w/2 \\ 0, & \text{otherwise.} \end{cases} \tag{18}$$

In the z-direction, the charge distribution will be more or less flat except near the edges. This prompts us to choose the following distribution for $g(z)$:

$$g(z) = \begin{cases} 1, & -(l/2-k) \leqslant z \leqslant (l/2-k) \\ 1 + \left(\dfrac{A}{k}\right)\left[|z| - (l/2-k)\right], & \\ \quad -l/2 \leqslant z \leqslant -(l/2-k) & \\ \qquad (l/2-k) \leqslant z \leqslant l/2 & \\ 0, \quad \text{otherwise.} & \end{cases} \tag{19}$$

A and k are constants determined by numerically maximizing the capacitance C_l. Fourier transforming (18) and (19) and evaluating (3) and (2), we get

$$f(\alpha,\beta) = f(\alpha)g(\beta) \tag{20}$$

where

$$f(\alpha) = \frac{5w}{4}\left\{1.6\left[\frac{\sin\left(\frac{\alpha w}{2}\right)}{\left(\frac{\alpha w}{2}\right)}\right] + \frac{2.4}{\left(\frac{\alpha w}{2}\right)^2}\left[\cos\left(\frac{\alpha w}{2}\right) - 2\left[\frac{\sin\left(\frac{\alpha w}{2}\right)}{\left(\frac{\alpha w}{2}\right)}\right] + \left[\frac{\sin\left(\frac{\alpha w}{4}\right)}{\left(\frac{\alpha w}{4}\right)}\right]^2\right]\right\} \tag{21}$$

$$g(\beta) = \frac{2}{\beta}(1+A)\sin\left(\frac{\beta l}{2}\right) - \left[\frac{4A}{k\beta^2}\left(\sin\left(\frac{\beta l - \beta k}{2}\right)\sin\left(\frac{\beta k}{2}\right)\right)\right] \tag{22}$$

$$Q = \frac{5w}{4}\left[Ak + l\right]. \tag{23}$$

Using (20)–(23) in (16), the line capacitance of the finite-length strip conductor embedded in multilayer dielectrics can be determined. Once C_l is determined, the edge-capacitance (C_{0c}) can be obtained as

$$C_{0c} = \lim_{l\to\infty} 0.5\left[C_l - lC\right] \tag{24}$$

where C_l is the capacitance of the section of length l and width w obtained from (16) and C is the line capacitance per unit length of a uniform line of the same width. The expression for C is already available in an earlier paper by the authors [2]. The edge-capacitance can also be expressed in terms of a hypothetical extension of the strip conductor by a small amount Δl which is given by

$$\Delta l = \frac{C_{0c}}{C}. \tag{25}$$

In evaluating (24), l is not infinite but some finitely large value beyond which the change in $(C_l - lC)$ is negligible. Expressions (16), (24), and (25) are general. For solving various microstrip-like structures, the only parameter to be determined is the admittance Y at the charge plane which can be obtained from the transverse transmission-line formulas. In this paper, a four-layer microstrip is analyzed. However, the same expressions are valid for N-layer microstrip using a modified admittance expression.

III. Numerical Results

A numerical experiment showed that for determining the lumped capacitance of square and rectangular conductor patches, a uniform charge distribution in the z-direction ($g(z) = 1$, $-l/2 \leqslant z \leqslant l/2$) gives quite accurate results adequate for most applications. Therefore, for determining the lumped capacitance of square and rectangular conductor patches in various microstrip-like configurations, the factor A appearing in (19) is set equal to zero. Further, for determining the open-circuit end effects and edge-capacitance, the factor A is set equal to 1. Fig. 3 illustrates the variations of normalized capacitance C_N of square and rectangular conductor patches in sandwiched microstrip as a function of b/w, for fixed values of a_1/b, a_2/b, ϵ_{r1}, and ϵ_{r2}. The normalizing factor is the parallel-plate capacitance of the conductor patch situated at a distance $(a_1 + b)$ in free space above the ground plane. This factor is $\epsilon_0 w^2/(a_1 + b)$ for the square patch and $\epsilon_0 w^2/2(a_1 + b)$ for the rectangular patch with $l = w/2$. As b/w increases, C_N increases. The values of C_N for the rectangular conductor patch are higher than with those for the square conductor patch. The variations of the normalized edge-capacitance (C_{0c}/w) and normalized extension in length due to end effects $(\Delta l/b)$ are plotted in Fig. 4 as a function of w/b, for fixed a_1/b, a_2/b, ϵ_{r1}, and ϵ_{r2}. As w/b increases,

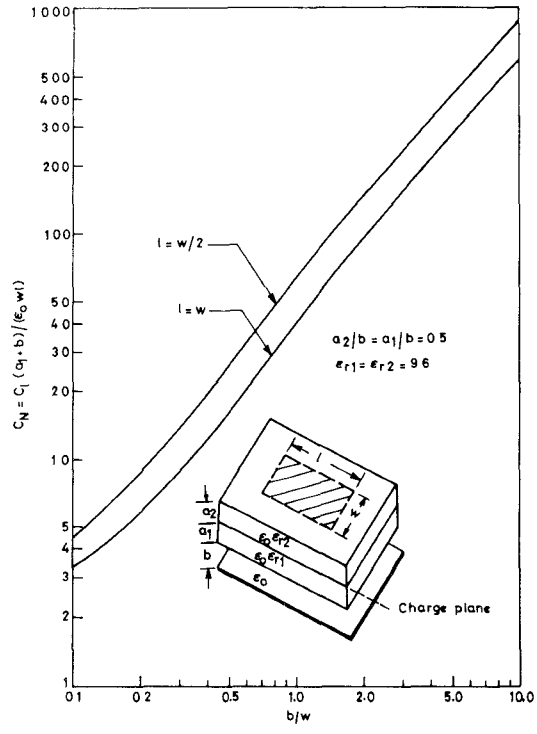

Fig. 3. Normalized capacitance of square and rectangular conductor patches in sandwiched microstrip versus air-gap height.

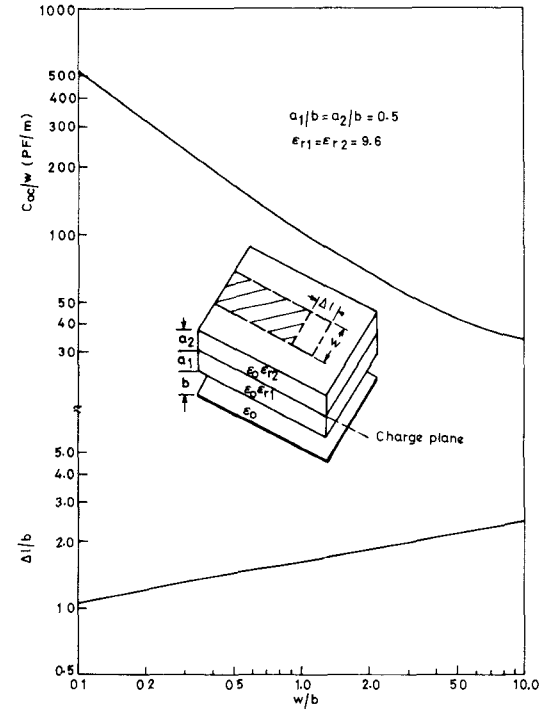

Fig. 4. Variations of normalized edge-capacitance and normalized extension in length of sandwiched microstrip versus strip width.

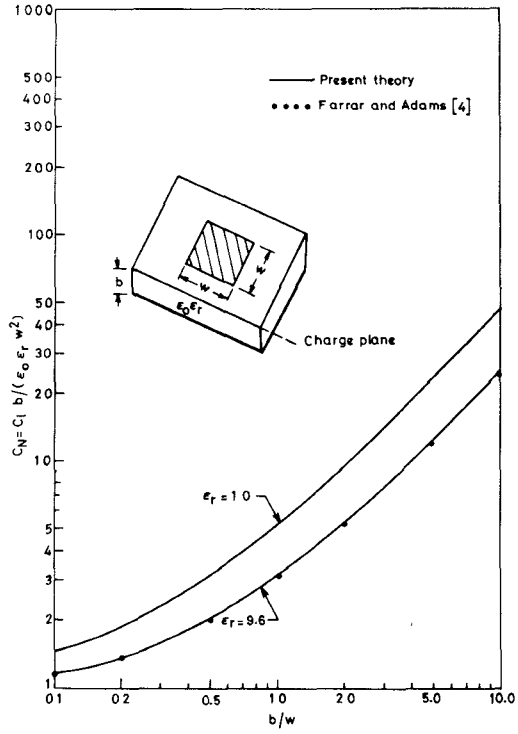

Fig. 5. Comparison of normalized capacitance of the square conductor patch in microstrip versus dielectric height using present theory with those reported by Farrar and Adams [4].

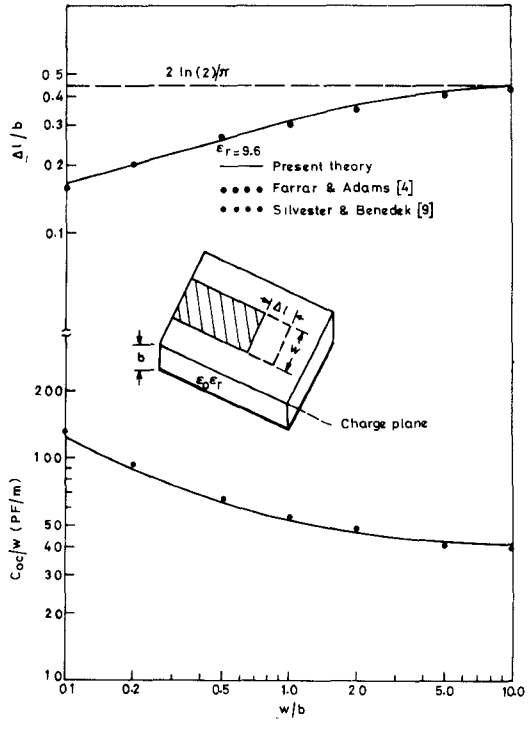

Fig. 6. Comparison of normalized edge-capacitance and normalized extension in length of microstrip versus strip width using present theory with those reported by other authors [4], [9].

C_{0c}/w decreases, whereas $\Delta l/b$ increases. It is observed that for the structural parameters considered, the extension in length due to end effects is of the order of 1.0 to 2.5 times the air-gap height.

As a numerical check, the lumped capacitance, open-circuit end effects, and edge-capacitance of the conventional microstrip structure in open configuration have been computed. Fig. 5 shows the variations of normalized capacitance C_N of the square conductor patch versus b/w. The variations of C_{0c}/w and $\Delta l/b$ versus w/b are plotted in Fig. 6. Superimposed on these graphs are the results reported by other authors [4], [9]. As can be seen, there is very good agreement between the results obtained using the present theory and those reported by other authors.

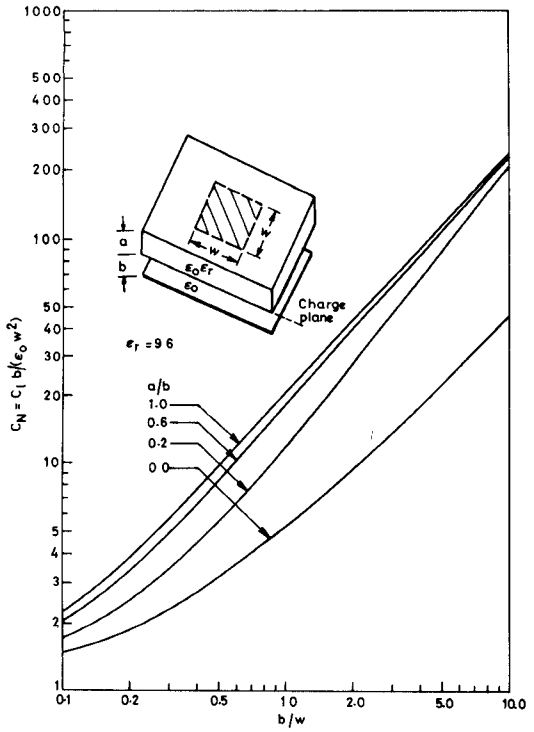

Fig. 7. Variations of normalized capacitance of the square conductor patch in inverted microstrip versus air-gap height with the thickness of the dielectric substrate as a parameter.

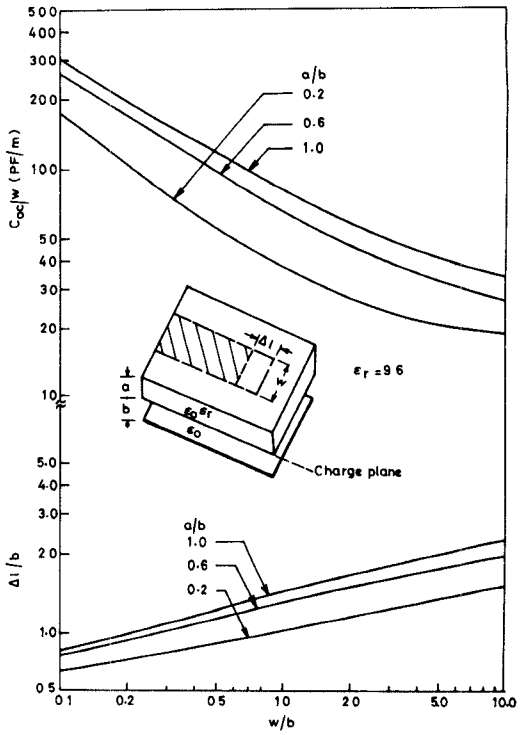

Fig. 9. Variations of normalized edge-capacitance and normalized extension in length of inverted microstrip versus strip width with the thickness of the dielectric substrate as a parameter.

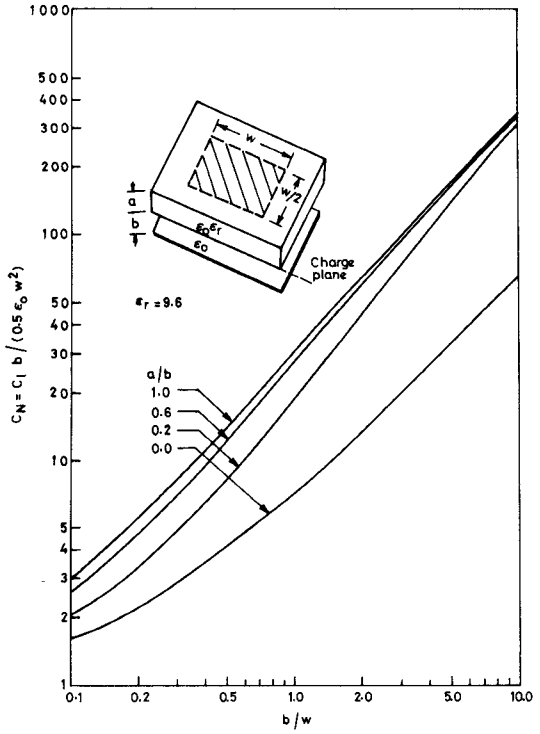

Fig. 8. Variations of normalized capacitance of the rectangular conductor patch in inverted microstrip versus air-gap height with the thickness of the dielectric substrate as a parameter.

The variations of normalized capacitance C_N of square and rectangular conductor patches in inverted microstrip as a function of b/w with a/b as a parameter are plotted in Figs. 7 and 8, respectively. The normalizing factor is the parallel-plate capacitance of the conductor patch situated at a distance b in free space above the ground plane. This factor is $\epsilon_0 w^2/b$ for the square patch and $\epsilon_0 w^2/2b$ for the rectangular patch with $l = w/2$. It is observed that C_N increases with an increase in a/b or b/w. The values of C_N obtained for the rectangular conductor patch are higher than those obtained for a square conductor patch. Fig. 9 depicts the variations of normalized edge-capacitance (C_{0c}/w) and normalized extension in length due to the end effects $(\Delta l/b)$ as a function of w/b, with a/b as a parameter. For a fixed value of a/b, $\Delta l/b$ increases and C_{0c}/w decreases with an increase in w/b. On the other hand, for a fixed value of w/b, both $\Delta l/b$ and C_{0c}/w increase as a/b is increased. For the structural parameters chosen, the extension in length of the line due to the end effects is of the order of 0.6 to 2.3 times the air-gap height. The values of Δl obtained in the present structure are considerably higher as compared with those obtained in the conventional microstrip.

Figs. 10 and 11 depict the variations of normalized capacitance C_N of square and rectangular conductor patches in suspended microstrip as a function of b/w with a/b as a parameter. The normalizing factor is the parallel-plate capacitance of the conductor patch situated at a distance $(a + b)$ in free space above the ground plane. This factor is $\epsilon_0 w^2/(a + b)$ for the square patch and $\epsilon_0 w^2/2(a + b)$ for the rectangular patch with $l = w/2$. Fig. 12 shows the variations of normalized edge-capacitance (C_{0c}/w) and the normalized extension in length due to end effects $(\Delta l/b)$ as a function of w/b, with a/b as a parameter. The variations obtained are similar to those obtained in the case of inverted microstrip. For the structural parameters chosen, the extension in length due to end effects is of the order of 0.6 to 2.4 times the air-gap height. Compared with

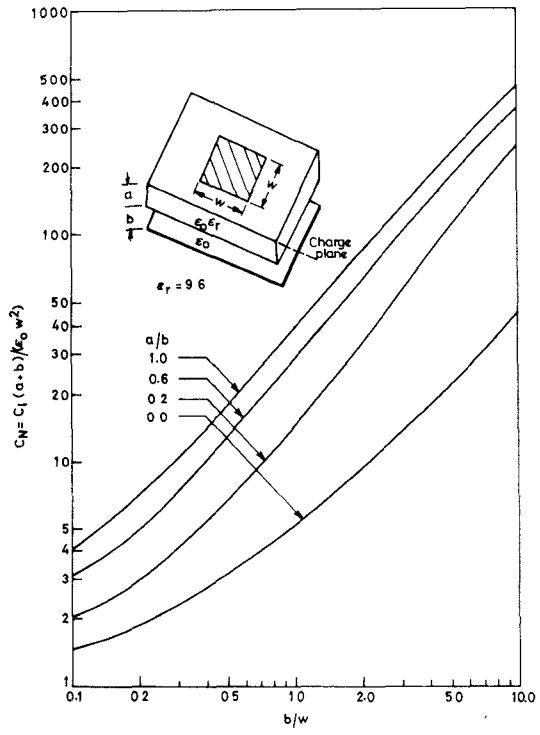

Fig. 10. Variations of normalized capacitance of the square conductor patch in suspended microstrip versus air-gap height with the thickness of the dielectric substrate as a parameter.

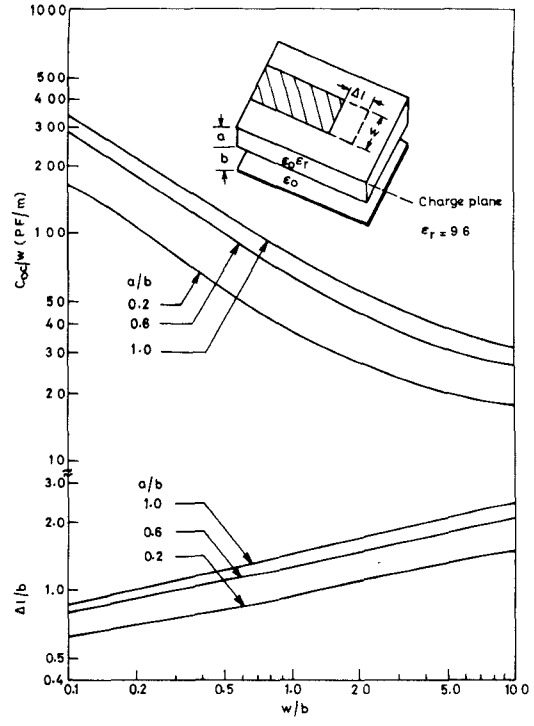

Fig. 12. Variations of normalized edge-capacitance and normalized extension in length of suspended microstrip versus strip width with the thickness of the dielectric substrate as a parameter.

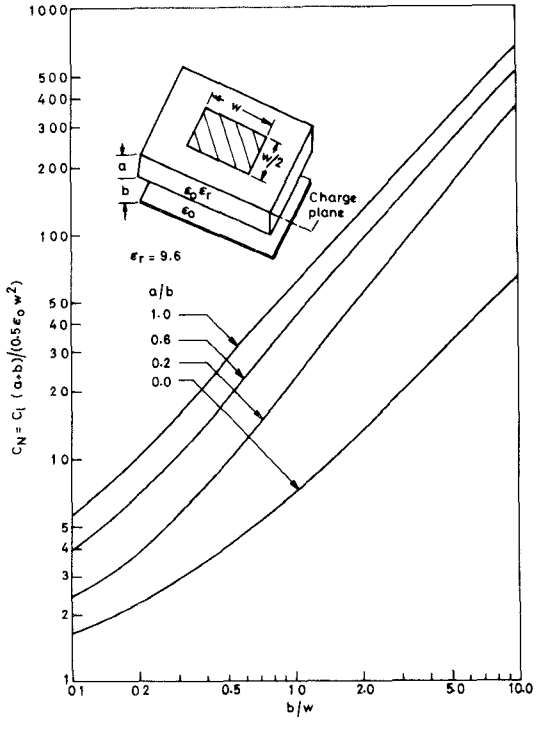

Fig. 11. Variations of normalized capacitance of the rectangular conductor patch in suspended microstrip versus air-gap height with the thickness of the dielectric substrate as a parameter.

the conventional microstrip, the values of Δl obtained in the present structure are considerably larger.

IV. Conclusions

The analysis of finite-length strip conductor in a multilayer microstrip structure is presented in this paper. Extensive design data on the lumped capacitances of square and rectangular conductor patches, open-circuit end effects, and edge-capacitances of a) sandwiched microstrip, b) inverted microstrip, and c) suspended microstrip are generated. Compared with the conventional microstripline, the values of Δl obtained in various microstrip-like configurations reported in this paper are higher. The design data presented should be very useful for designing lumped elements and filters in sandwiched microstrip, inverted microstrip, and suspended microstrip.

The analysis of a finite-length strip conductor embedded in multilayer isotropic dielectric substrates presented is fairly general. A variety of structures can be analyzed by simply determining the admittance parameter.

References

[1] I. Wolff, MIC-Bibliography, Verlag H. Wolff, Benedikitinerweg, Aachen, Germany, 1979.

[2] S. K. Koul and B. Bhat, "Characteristic impedance of microstrip-like transmission lines for millimeter wave applications," *Arch. Elek. Übertragung*, vol. 35, pp. 253–258, June 1981.

[3] S. K Koul and B. Bhat, "Propagation parameters of coupled microstrip-like transmission lines for millimeter-wave applications," *IEEE Trans. Microwave Theory Tech.*, vol. MTT-29, pp. 1364–1370, Dec. 1981.

[4] A. Farrar and A. T. Adams, "Computation of lumped microstrip capacities by matrix methods. Rectangular sections and end effects," *IEEE Trans. Microwave Theory Tech.*, vol. MTT-19, pp. 495–497, May 1971; also "Correction," *IEEE Trans. Microwave Theory Tech.*, vol. MTT-20, p. 294, Apr. 1972.

[5] T. Itoh, R. Mittra, and R. D. Ward, "A method for computing edge capacitance of finite and semi-infinite microstrip lines," *IEEE Trans. Microwave Theory Tech.*, vol. MTT-20, pp. 847–849, Dec. 1972.

[6] S. S. Bedair and M I. Sobhy, "Open-end discontinuity in shielded microstrip circuits," *IEEE Trans. Microwave Theory Tech.*, vol MTT-29, pp. 1107–1109, Oct. 1981.

[7] H. M. Altschuler and A. A. Oliner, "Discontinuities in the centre conductor of symmetric strip transmission line," *IRE Trans. Micro-*

wave Theory Tech., vol. MTT-8, pp. 328–329, May 1960.
[8] M. Maeda, "An analysis of gap in microstrip transmission lines," *IEEE Trans. Microwave Theory Tech.*, vol. MTT-20, pp. 390–396, June 1972.
[9] P. Silvester and P. Benedek, "Equivalent capacitances of microstrip open circuit," *IEEE Trans. Microwave Theory Tech.*, vol. MTT-20, pp. 511–516, Aug. 1972.
[10] D. S. James and S. H. Tse, "Microstrip end effects," *Electron. Lett.*, vol. 8, pp. 46–47, Jan. 1972.
[11] J. S. Hornsby, "Full wave analysis of microstrip resonators and open-circuit end effects," *Proc. Inst. Elec. Eng., Microwaves, Optics and Antennas*, part H, vol. 129, pp. 338–341, Dec. 1982.
[12] R. H. Jansen, "Hybrid mode analysis of end effects of planar microwave and millimeter-wave transmission lines," *Proc. Inst. Elec. Eng., Microwaves, Optics and Antennas*, part H, vol. 128, pp. 77–86, Apr. 1981.
[13] L. S. Napoli and J. J. Hughes, "Foreshortening of microstrip open-circuit on alumina substrates," *IEEE Trans. Microwave Theory Tech.*, vol. MTT-19, pp. 559–561, June 1971.
[14] B. Easter, A. Gopinath, and I. M. Stephenson, "Theoretical and experimental methods for evaluating discontinuities in microstrip," *Radio Electron Eng.*, vol. 48, pp. 73–84, Jan./Feb. 1978.

Bharathi Bhat (SM'82) received the B.E. degree in electrical communication engineering and the M.E. degree in electronics, both with distinction, from the Indian Institute of Science, Bangalore, India, in 1963 and 1965, respectively. She continued her graduate studies at Harvard University, Cambridge, MA, and received the M.S. and Ph.D degrees from the Division of Engineering and Applied Physics in 1967 and 1971, respectively.

From 1971 to 1972, she worked as a Post-Doctoral Research Fellow in the Division of Engineering and Applied Physics, Harvard University. In 1973, she joined the Indian Institute of Technology, New Delhi, as an Assistant Professor. Since 1977, she has been a Professor at the Centre for Applied Research in Electronics (CARE). During the period 1979–1982, she was the Head of CARE, IIT, New Delhi. She is also the leader of the Microwave Group in CARE, and has been directing a number of sponsored research projects in the areas of microwave antennas, electronic phase shifters, and microwave and millimeter-wave integrated circuits and components.

Dr. Bhat is a Fellow of the Institution of Electronics and Telecommunication Engineers (IETE), India. She has been the Honorary Editor of the IETE Journal (electromagnetics section) since January 1981, and a member of the IETE Council since January 1982. She is presently the Chairman of the ED/MTT Chapter of the IEEE India Council.

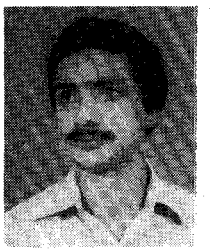

Shiban Kishen Koul (S'81–M'83) received the Bachelor of Engineering degree in electrical engineering from the Regional Engineering College, Srinagar, J&K, India, in 1977, and the Master of Technology degree in radar and communications engineering, with distinction, from the Indian Institute of Technology (IIT), Delhi, India, in 1979.

From 1979 to 1980, he worked as a Senior Research Assistant in the Centre for Applied Research in Electronics (CARE) at the Indian Institute of Technology, Delhi. Since 1980, he has been a Senior Scientific Officer in CARE. He entered the Ph.D program as a part-time student, in January 1980, and has recently received the Ph.D degree. He is presently engaged in research in the areas of thin-film microwave integrated circuits, microstrip-like transmission lines, ferrite phase shifters, and millimeter-wave transmission lines.

Multiconductor Transmission Lines in Multilayered Dielectric Media

CAO WEI, ROGER F. HARRINGTON, FELLOW, IEEE, JOSEPH R. MAUTZ, SENIOR MEMBER, IEEE, AND TAPAN K. SARKAR, SENIOR MEMBER, IEEE

***Abstract*—A method for computing the capacitance matrix and inductance matrix for a multiconductor transmission line in a multilayered dielectric region is presented. The number of conductors and the number of dielectric layers are arbitrary. Some of the conductors may be of finite cross section and others may be infinitesimally thin. The conductors are either above a single ground plane or between two parallel ground planes. The formulation is obtained by using a free-space Green's function in conjunction with total charge on the conductor-to-dielectric interfaces and polarization charge on the dielectric-to-dielectric interfaces. The solution is effected by the method of moments using pulses for expansion and point matching for testing. Computed results are given for some cases where all conducting lines are of finite cross section and other cases where they are infinitesimally thin.**

Manuscript received September 26, 1983; revised November 7, 1983. This work was supported in part by the Digital Equipment Corporation, Marlboro, MA.

C. Wei is a Visiting Scientist at Syracuse University, on leave from the Nanjing Institute of Posts and Telecommunications, China.

R. F. Harrington and J. R. Mautz are with the Department of Electrical and Computer Engineering, Syracuse University, Syracuse, NY 13210.

T. K. Sarkar is with the Department of Electrical Engineering, Rochester Institute of Technology, Rochester, NY 14623.

I. INTRODUCTION

THE OBJECTIVE of this analysis is to determine the capacitance matrix and the inductance matrix of a multiconductor transmission-line system. Some of the con-

0018-9480/84/0400-0439$01.00 ©1984 IEEE